

Numerical analysis and optimization of gain lever and distortion in 1.3 μm bisection quantum well laser diode for 2.4 GHz radio over fiber applications

S. PIRAMASUBRAMANIAN*, M. GANESH MADHAN

Department of Electronics Engineering, Madras Institute of Technology Campus, Anna University, Chennai, India, 600 044

We analyze the distortion characteristics of 1.3 μm , gain levered multiple quantum well Laser, for 2.4 GHz radio over fiber applications. The rate equations are numerically solved to determine the device characteristics. Gain lever and second harmonic distortion are evaluated for different bias currents and section length ratios. First and second harmonic contents of optical power output are evaluated from this numerical solution. Further, mathematical expression for second harmonic distortion is also derived from the rate equations. Optimum values of device parameters and operating conditions for maximum gain lever and minimum distortion are determined.

(Received August 14, 2012; accepted January 22, 2014)

Keywords: Bi section MQW laser, Radio over Fiber (RoF), Gain lever effect, Second harmonic distortion, Third order intermodulation distortion, Runge – Kutta method, Rate equations

1. Introduction

Fiber optic analog links are finding increased importance in the areas of WLAN signal transmission, CATV, cellular mobile communication networks, phased array antennas and antenna remoting. The major limitation in the analog fiber optic link performance is its low RF link efficiency. The RF link loss in a typical DFB laser based single mode fiber link is around 30dB [1]. In order to overcome this loss and to improve the signal quality, RF amplifiers are needed prior to the laser diode in the transmitter and after photo detector in the receiver [2]. An alternate approach for increasing the signal quality and SNR is by enhancing the modulation efficiency of the laser diode. Gain lever effect is one scheme by which modulation efficiency can be improved in two section MQW laser diodes [3-8]. Two section laser diode can exhibit bistability, and self pulsation phenomenon, apart from gain lever effect [9-10]. Optical gain lever effect was first analyzed by Vahala

et al. [4] in two section quantum well laser. Gain lever effect in bulk and multiple quantum well lasers was demonstrated by Seltzer et al. [8]. For a laser diode, to exhibit gain lever effect, the active region has to be divided in to two unequal sections. RF current is given to the shorter section of laser diode and the longer section is DC biased at high gain level. The detailed rate equation analysis of gain lever single quantum well GaAlAs laser diode was provided by Moore et al [5]. Improvement in modulation efficiency in gain levered long wavelength InGaAsP/InP lasers was reported at a frequency of 900MHz, by Seltzer et al [6]. Gain lever phenomenon results due to the non linear transfer characteristic of laser diode. But it also introduces harmonic and inter

modulation distortion at higher modulation frequencies. This is an undesirable phenomenon that restricts the wide spread use of such devices in analog fiber optic links, in spite of its improved modulation efficiency. Earlier, inter modulation distortion and non linearity in conventional directly modulated single section laser diodes, were investigated by many authors [11-12], the most detail one is by Way [12]. Based on this approach, studies have been carried out to evaluate the intermodulation free dynamic range of gain lever lasers. For e.g. Westbrook et al.[7] reports the intermodulation free dynamic range of InGaAs/InP gain lever lasers in 900 MHz analog fiber optic link, where the effect of short section bias current with the constant section ratio is analyzed. Recently, reduction in harmonic distortion (2HD) and third order intermodulation distortion (IMD3) in gain lever DBR laser diode, by optical injection locking method, was reported by Sung et al.[13]. In this method, a number of devices are used in optical transmitter thereby increasing its complexity. Further, a modified laser diode structure for improved modulation performance along with reduced non linear distortion was reported by Rana et al. [14]. Harmonic content of optical power and resonant frequency for simple laser diode from the direct solution of rate equations are reported by Zandi et al. [15]. Recently, the 2.4 GHz ISM band has received considerable attention for WLAN and other applications. Subsequently, studies on radio over fiber links for the transport of 2.4 GHz wireless signals, has gained momentum. Direct RF modulation of 1.3 μm laser diodes is preferred for simple low cost RoF links. It is envisaged that incorporating gain levered laser diode for 2.4 GHz RoF link may improve the performance. However, detailed investigations on the device parameter and operating conditions on the gain lever and distortion

performance at 2.4 GHz band remain sparse. Hence, we investigate the gain lever performance at 2.4 GHz in a 1.3 μm MQW laser diode. The rate equation model is used to evaluate the gain lever dependence on bias currents and device section lengths. These rate equations are solved by direct method by extending the approach of Zandi et al. [15] for gain lever case. The numerical technique is based on Runge-Kutta method. Further, second harmonic distortion (2HD) and third order inter modulation distortion (IMD3) are analyzed for different section lengths under different bias currents at 2.4 GHz. The second harmonic distortion is compared for both direct and numerical solution of rate equations.

2. Gain lever laser diode model

A two section laser diode with unequal active region length is considered for the study. The structure has a longer section of length, a_1 , and a shorter section of length, a_2 , as shown in Fig. 1. The sections are electrically isolated and optically connected. RF signal (I_{RF}) along with bias current (I_a) is applied to the shorter section, DC current (I_g) is applied to longer section. The longer section is biased at higher gain level than the shorter section. At lasing threshold, total optical gain overcomes the loss of the cavity. An increase in gain in one section of the laser diode allows equal decrease in gain in other section. When current in shorter section, I_a decreases, the circulating optical power decreases, which results in increase of carrier density N_g in other section. The relation between optical gain and carrier density is sub linear. Hence a small amount of increase in carrier density N_g results in AM efficiency enhancement in such multi section laser diodes [4-5].

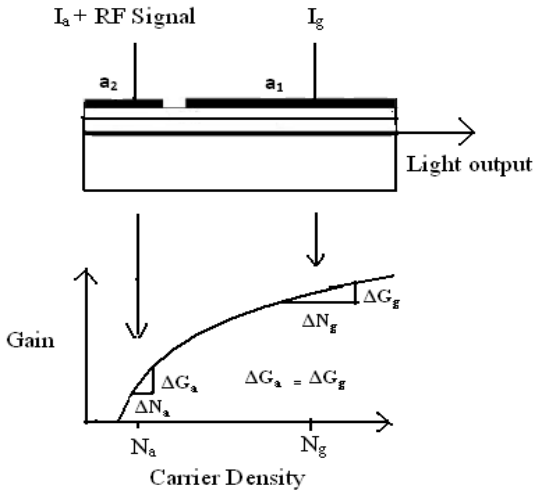


Fig. 1. Schematic diagram of Bi section gain lever laser diode.

The rate equations for the two section laser diode are as follows: [9 - 10]

$$\frac{dN_g}{dt} = \frac{I_g}{a_1 q V} - \frac{N_g}{\tau_g} - v_g g_g (N_g - N_{og}) S (1 - \epsilon S) - \frac{N_g}{\tau_{nr}} \quad (1)$$

$$\frac{dN_a}{dt} = \frac{I_a}{a_2 q V} - \frac{N_a}{\tau_a} - v_g g_a (N_a - N_{oa}) S (1 - \epsilon S) - \frac{N_a}{\tau_{nr}} \quad (2)$$

$$\frac{dS}{dt} = -\frac{S}{\tau_p} + [a_1 v_g g_g (N_g - N_{og}) + a_2 v_g g_a (N_a - N_{oa})] \Gamma S (1 - \epsilon S) + \Gamma \beta \left(\frac{a_1 N_g}{\tau_g} + \frac{a_2 N_a}{\tau_a} \right) \quad (3)$$

$$\tau_g = \frac{1}{(BN_g)}, \quad \tau_a = \frac{1}{(BN_a)} \quad (4)$$

Where ' N_g ', ' N_a ' are the carrier densities in section length ' a_1 ' and ' a_2 ' respectively. The total photon density is ' S ' and the total volume of active region is denoted by ' V '.

The longer section of bisection laser diode is injected with constant DC current. The following analysis is carried out by extending the scheme proposed by Zandi et al. [15], for gain lever case. The current injected into the shorter section is given by,

$$I_a = I_{a0} + I_{a1} e^{j\omega t} \quad (5)$$

The Fourier series representation of carrier density and photon density are given by [15],

$$N_a = \sum_{m=0}^{\infty} N_{am} e^{j\omega m t} \quad (6)$$

$$S = \sum_{m=0}^{\infty} S_m e^{j\omega m t} \quad (7)$$

After substituting the equations (5), (6) and (7) in equations (1), (2) and (3), the rate equations are modified as, ($\epsilon = 0$)

$$\frac{I_g}{a_1 q V} - \frac{N_g}{\tau_g} - v_g g_g (N_g - N_{og}) \sum_{m=0}^{\infty} S_m e^{j\omega m t} - \frac{N_g}{\tau_{nr}} = 0 \quad (8)$$

$$\sum_{m=0}^{\infty} N_{am} (j\omega m) e^{j\omega m t} = \frac{(I_{a0} + I_{a1} e^{j\omega t})}{a_2 q V} - \frac{1}{\tau_a} \sum_{m=0}^{\infty} N_{am} e^{j\omega m t} - v_g g_a \left(\sum_{m=0}^{\infty} N_{am} e^{j\omega m t} - N_{oa} \right) \sum_{m=0}^{\infty} S_m e^{j\omega m t} - \frac{1}{\tau_{nr}} \sum_{m=0}^{\infty} N_{am} e^{j\omega m t} \quad (9)$$

$$\sum_{m=0}^{\infty} S_m (j\omega m) e^{j\omega m t} = -\frac{1}{\tau_p} \sum_{m=0}^{\infty} S_m e^{j\omega m t} + [a_1 v_g g_g (N_g - N_{og}) + a_2 v_g g_a \left(\sum_{m=0}^{\infty} N_{am} e^{j\omega m t} - N_{oa} \right)] \Gamma \sum_{m=0}^{\infty} S_m e^{j\omega m t} + \Gamma \beta \left(\frac{a_1 N_g}{\tau_g} + \frac{a_2}{\tau_a} \sum_{m=0}^{\infty} N_{am} e^{j\omega m t} \right) \quad (10)$$

For the DC analysis ($m = 0$), the following expressions for carrier and photon densities are obtained.

$$N_g = \frac{\left(\frac{I_g}{a_1 q V}\right) + v_g g_g N_{og} S_0}{\left(\frac{1}{\tau_g} + \frac{1}{\tau_{nr}} + v_g g_g S_0\right)} \quad (11)$$

$$N_{a0} = \frac{\left(\frac{I_{a0}}{a_2 q V}\right) - v_g g_a N_{a0} S_1 + v_g g_a N_{oa} S_1}{\left(j\omega + v_g g_a S_0 \frac{1}{\tau_a} + \frac{1}{\tau_{nr}}\right)} \quad (12)$$

$$S_0 = \frac{\Gamma \beta \left(\frac{a_1 N_g}{\tau_g} + \frac{a_2 N_a}{\tau_a}\right)}{\frac{1}{\tau_p} - [a_1 v_g g_g (N_g - N_{og}) + a_2 v_g g_a (N_a - N_{oa})] \Gamma} \quad (13)$$

Similarly the first harmonic terms of shorter section carrier density and photon density can be obtained from above equations by substituting $m = 1$.

$$N_{a1} = \frac{\left(\frac{I_{a1}}{a_2 q V}\right) - v_g g_a N_{a0} S_1 + v_g g_a N_{oa} S_1}{\left(j\omega + v_g g_a S_0 + \frac{1}{\tau_a} + \frac{1}{\tau_{nr}}\right)} \quad (14)$$

$$S_1 = \frac{(a_2 v_g g_a N_{a1} S_0 \Gamma + \Gamma \beta \left(\frac{a_2 N_{a1}}{\tau_a}\right))}{\left(j\omega + \frac{1}{\tau_p} - a_1 v_g g_g (N_g - N_{og}) \Gamma - a_2 v_g g_a N_{a0} \Gamma + a_2 v_g g_a N_{oa} \Gamma\right)} \quad (15)$$

The second harmonic content of carrier density and photon density are obtained as

$$N_{a2} = \frac{(-v_g g_a N_{a0} S_2 - v_g g_a N_{a1} S_1 + v_g g_a N_{oa} S_2)}{\left(2j\omega + v_g g_a S_0 + \frac{1}{\tau_a} + \frac{1}{\tau_{nr}}\right)} \quad (16)$$

$$S_2 = \frac{(a_2 v_g g_a N_{a1} S_1 \Gamma + a_2 v_g g_a N_{a2} S_0 \Gamma + \Gamma \beta \left(\frac{a_2 N_{a2}}{\tau_a}\right))}{\left(2j\omega + \frac{1}{\tau_p} - a_1 v_g g_g (N_g - N_{og}) \Gamma - a_2 v_g g_a N_{a0} \Gamma + a_2 v_g g_a N_{oa} \Gamma\right)} \quad (17)$$

The optical power output is calculated from photon density by the following equation,

$$P_n = \frac{chV\eta}{\Gamma \tau_p \lambda} S_n, \quad n = 0, 1, 2 \dots \quad (18)$$

3. Effect of bias current on gain lever and distortion

For static conditions, left hand side of equations (1), (2) and (3) are made equal to zero and the solutions are obtained for carrier densities and photon density, with respect to applied injection currents, in the respective sections. Codes were written in MATLAB[®] to solve the equations (1) to (4), by Runge-Kutta method and the laser diode characteristics are determined. These static results are compared with the characteristics of unlevered laser, where both sections are shorted. The static characteristic of unlevered laser is plotted with bias currents varied from 0-100 mA. This is realized by providing equal currents, (0-50 mA) to both sections. In the following sections, we present the DC and modulation characteristics of the two section laser with different section length ratios and compare with unlevered case. The device parameters used in this work are similar to that of Ref [9] and they are given in table 1. An internal quantum efficiency of 0.1 is considered for the analysis.

Table 1. Device parameters [9].

Description	Value
Number of quantum wells	6
V, total volume of active region of laser diode	$48.52 \times 10^{-12} \text{ cm}^3$
q, charge of the electron	$1.603 \times 10^{-19} \text{ C}$
τ_a , carrier life time –shorter section	1ns
τ_g , carrier life time –longer section	1ns
τ_{nr} , non radiative recombination time	1ns
g_a , gain constant-shorter section	$80 \times 10^{-16} \text{ cm}^2$
g_g , gain constant-longer section	$2 \times 10^{-16} \text{ cm}^2$
N_{oa} , transparency carrier density–shorter section	$1.25 \times 10^{18} \text{ cm}^{-3}$
N_{og} , transparency carrier density-longer section	$1.25 \times 10^{18} \text{ cm}^{-3}$
τ_p , photon life time	1.87 ps
a_1 , section length ratio – longer section	0.6,0.65,0.7,0.72, 0.75,0.78, 0.8,0.9,0.97
a_2 , section length ratio- shorter section	(1 - a_1)
β , coupling coefficient	1×10^{-5}
B, Bimolecular recombination coefficient	$1 \times 10^{-10} \text{ cm}^3/\text{s}$
Γ , Optical confinement factor	0.15
ϵ , Gain compression factor	$2 \times 10^{-17} \text{ cm}^3$
V_g , Group velocity	$0.85714 \times 10^{10} \text{ cm/s}$

3.1. Static characteristics for a section length ratio of (97/03)

In this simulation, the longer section current is varied from 0-100 mA and the output power is plotted. A threshold current of 52 mA is obtained when $I_a = 0$ (un pumped). The threshold current is found to reduce, when the shorter section is electrically pumped. The P-I characteristics for shorter section current, $I_a = 0$ and $I_a = 1$ mA is shown in Fig. 2. This result agrees with the experimental results of Uenohara et al. [9] and hence validates our procedure.

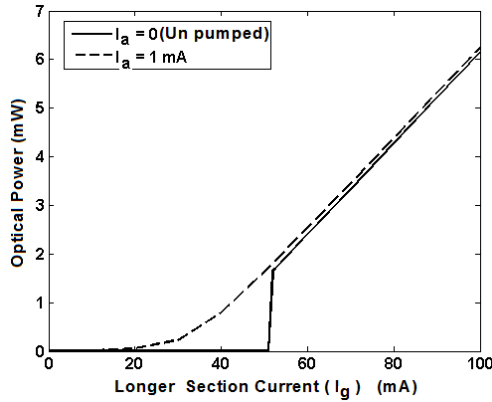


Fig. 2. Static characteristic of bi section MQW laser diode with section length ratio (97/03).

3.2. Effect of bias currents on the AM efficiency and distortion for the length ratio of (90/10)

Gain lever or AM enhancement is a strong function of applied bias current. For obtaining the characteristics of laser diode with section length ratio (90/10), the values for a_1 and a_2 are fixed as 0.9 and 0.1 respectively, in the rate equations. In this analysis, the current in shorter section (I_a) is varied from 0 to 15 mA with a constant current (I_g) applied to the longer section. The static characteristics (P vs I) of gain lever laser diode is shown in Fig. 3.

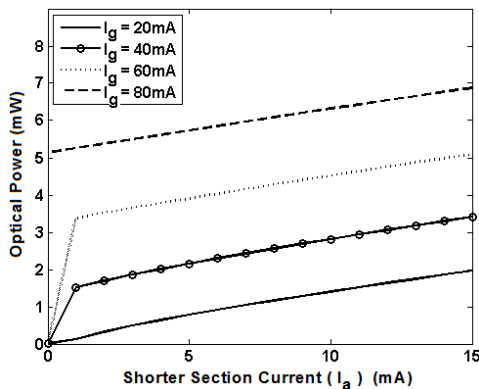


Fig. 3. Static characteristic of gain levered MQW laser diode with section length ratio (90/10).

It is observed that the threshold current of the device reduces for increasing values of longer section current (I_g). Slope efficiency (W/A) is found to be higher than unlevered laser, where both the sections are shorted. The above results agree well with finding of Pocha et.al.[3] and hence validates our simulation methodology.

To evaluate the gain lever and distortion performance at 2.4 GHz, a 3 mA RF signal is provided along with the DC current (I_a) to the shorter section. The DC bias current (I_a) is varied from 5 mA to 14 mA and the gain lever is evaluated for different values of longer section current (I_g). For the calculation of AM efficiency in unlevered case, a 2.4 GHz RF current at 1.5 mA is applied to shorted section ($I_a = I_g$). Gain lever or AM enhancement is calculated as the ratio of AM efficiency for RF signal in two section laser diode to the same as in unlevered laser diode.

$$GL = \frac{(P_{max}/P_{min})}{(P_{max}/P_{min})_{shorted}} \quad (19)$$

Where ' P_{max} ' and ' P_{min} ', correspond to the maximum and minimum values of optical power output under sinusoidal RF current input. The gain lever values calculated for various values of I_g are plotted in Fig. 4. In general, for two section gain lever laser diodes, a small DC bias current with 2.4 GHz RF is applied to shorter section and large value of DC bias current is applied to the longer section. The value of gain constant is higher for shorter section compared to the longer section. Gain lever is directly proportional to the ratio of gain constant of shorter section to that of longer section. Further, gain lever is maximum when the device is biased near to the threshold current of the device [4-6]. This bias point mainly depends on shorter section current.

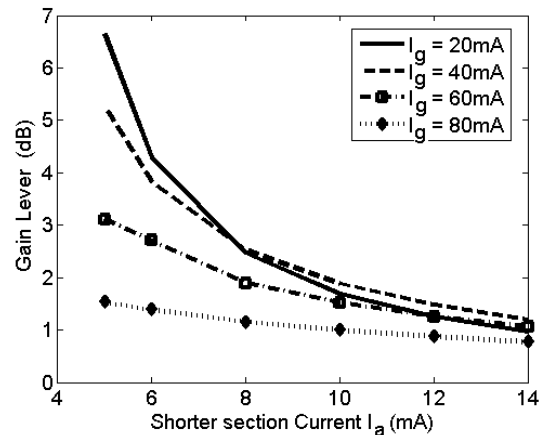


Fig. 4. Gain Lever (AM efficiency enhancement) variation with shorter section current (I_a) at 2.4 GHz.

The shorter section current should be fixed close to the threshold in order to get the maximum gain lever. However, the device nonlinearity is also higher at this condition. Further, the optical power is low when

compared to higher bias currents. The shorter section current is varied from 5 mA to 14 mA, for a constant longer section bias of 20 mA, 40 mA, 60 mA and 80 mA. The shorter section threshold current is 1.4 mA for 20 mA and it is reduced to 0.6 mA at the longer section current of 80 mA. Gain lever is maximum at 20 mA longer section current and exponentially decreases with shorter section current. Similar results are observed by Seltzer et al [8]. From the above graph, a maximum gain lever of 6.65 dB is obtained, which corresponds to the DC bias conditions of $I_a = 5\text{mA}$ and $I_g = 20\text{mA}$. It is found that AM enhancement tends to decrease for higher value of bias currents. Gain lever is exponentially proportional to shorter section current I_a in the region near threshold current. Gain lever decreases with increase in I_a .

The second harmonic distortion (2HD) is calculated as the ratio of optical power at 4.8 GHz to the fundamental signal power at 2.4 GHz. The distortion is evaluated with respect to short section current (I_a) at different levels of I_g , and plotted in Fig. 5. A minimum value of -21.76 dBc is obtained for bias currents $I_a = 14\text{mA}$, $I_g = 20\text{mA}$ for this section ratio. The 2HD is found to decrease with increasing short section current, as in the case of simple laser diode.

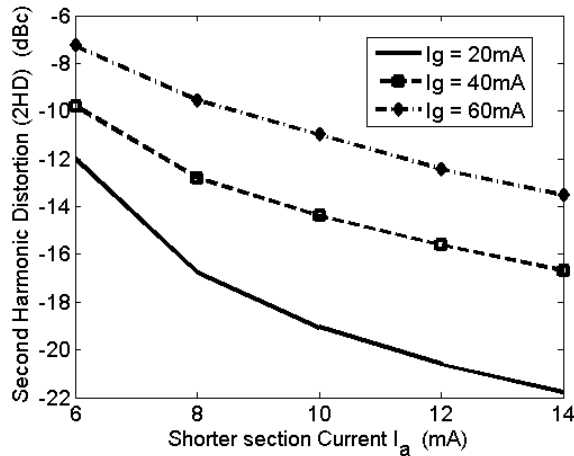


Fig. 5. Second order harmonic distortion (2HD) with shorter section Current (I_a) at 2.4 GHz.

Third order inter modulation distortion (IMD3) is calculated by providing two single tone frequencies $f_1 = 2.35\text{GHz}$ and $f_2 = 2.25\text{GHz}$, to the shorter section at 3mA RF current (I_a) and evaluating the optical output power at 2.45 GHz ($2f_1 - f_2$) and 2.15 GHz ($2f_2 - f_1$). The effect of DC bias point at the shorter and longer section on the inter modulation distortion is studied by varying the shorter section bias current from 6mA to 14mA, at fixed longer section currents. The plot in Fig. 6 shows a reduction of IMD3 with this bias current.

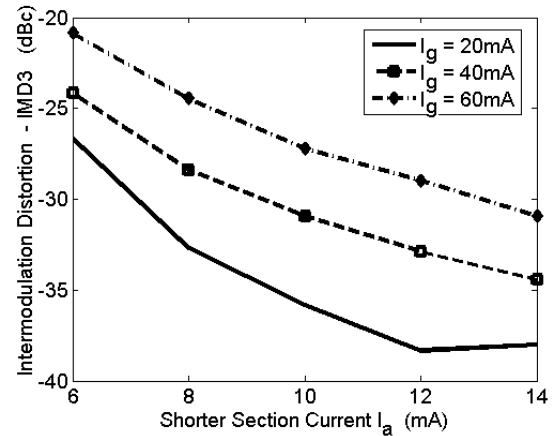


Fig. 6. Third order Inter modulation distortion (IMD3) with shorter section current (I_a) at $f_1 = 2.35\text{GHz}$, $f_2 = 2.25\text{GHz}$.

4. Effect of section lengths on gain lever and distortion

4.1. Analysis of gain lever and distortion for different section lengths

In order to investigate the effect of active region section lengths on gain lever and distortion, the static characteristics are first evaluated for section length ratios (a_1/a_2) of (90/10), (80/20), (70/30) and (60/40). Optical power output is also calculated for the variation in shorter active section (I_a) current at a constant gain section (I_g) current. The same biasing conditions are selected for all devices in order to compare the results obtained by Pocha et al [3]. The shorter section threshold current is found for different section lengths under different longer section bias currents (Fig. 7). A minimum threshold current is obtained for the section length ratio of (90/10). These results are in agreement with the literature, thereby validating our model [3].

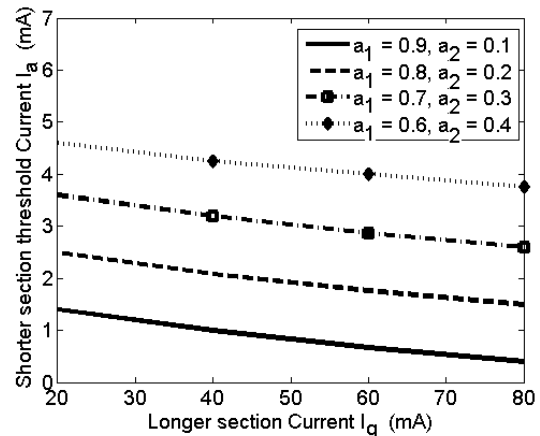


Fig. 7. Shorter section threshold current (I_{ath}) for different section lengths.

Based on the static characteristics, the bias points are fixed and frequency response is obtained for different section lengths, and is plotted in Fig. 8a. For this analysis, the bias currents are fixed at 20 mA (I_g) and 8 mA (I_{a0} (DC)) for longer and shorter sections respectively. The magnitude of RF current is 3 mA (I_{a1}). The choice of above mentioned bias point and RF current is mainly due to the value of maximum shorter section threshold current (4.6 mA), for the section length ratio of (60/40). This bias point is very close to threshold current I_a of section length ratio (60/40). The maximum gain lever and distortion are also obtained for this section length ratio (60/40), because of this threshold current value. The gain lever and distortion are also minimum for section length ratio of (90/10), as the bias current is 5 times larger than this threshold current. The same operating condition is maintained to evaluate the effect of section length ratio on the device performance. The shorter section threshold currents for section length ratio (90/10), (80/20), (70/30) and (60/40) are 1.4 mA, 2.4 mA, 3.6 mA and 4.6 mA respectively (Fig. 7). The section length ratio is varied from (90/10) to (60/40). The above values of currents are substituted into rate equations and numerically solved. The frequency is varied from 100 MHz to 30 GHz and optical power is evaluated for each value of frequency. The amplitude modulation efficiency (P_{max} / P_{min}) is calculated for each value of frequency and plotted for all four section length ratios.

An additional resonant peak is observed in the frequency response near to the device peak resonant frequency (Fig. 8a) [16]. This is mainly due to the choice of bias current and subsequent distortion. The harmonic distortion is more for the section length ratio of (60/40). This distortion reduces with increase in section length ratio. This is observed from the fact that the magnitude of additional resonant peak is low for section length ratio (90/10). The frequency response for the unlevered cases (60/40 and 90/10) are evaluated by providing a RF current of 1.5 mA with a DC bias of 14 mA injected into both sections ($I_a = I_g$) and plotted in Fig. 8b. AM efficiency and distortion are low for unlevered case. The additional resonant peak is not observed in the frequency response of unlevered laser diode. The bias current is larger than the threshold current of unlevered laser diode. From the results, modulation bandwidth and peak resonant frequency are also evaluated and plotted in Fig. 9.

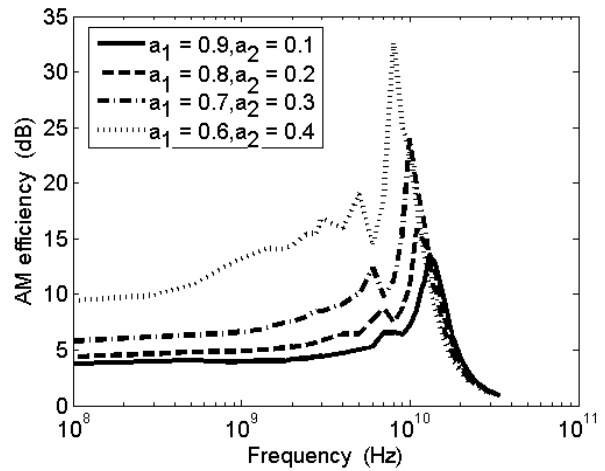


Fig. 8a. Frequency Response of Gain Lever Laser diode for bias current at $I_g = 20$ mA and $I_a = 8$ mA.

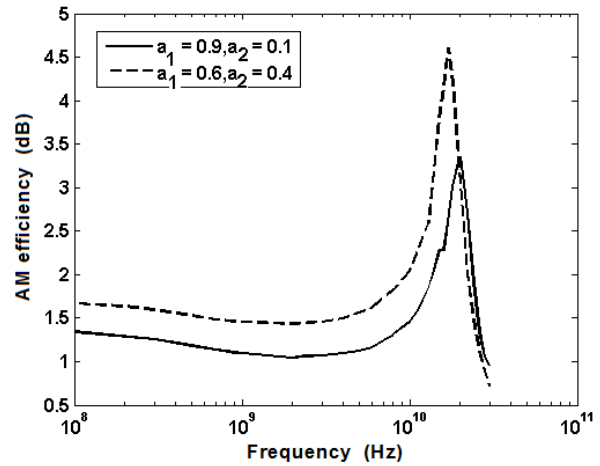


Fig. 8b. Frequency Response of Gain Lever Laser diode for bias current at $I_g = I_a = 14$ mA and $I_{a1} = 1.5$ mA.

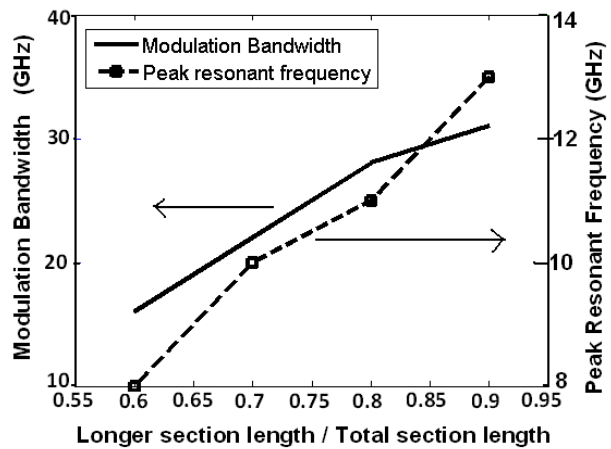


Fig. 9. Modulation Bandwidth and peak resonant frequency variation with section lengths.

From the above graph, an improved bandwidth (31 GHz) is observed for (90/10) section ratio, whereas the (60/40) case shows a bandwidth of 16 GHz only. The frequency response for the unlevered case is evaluated by a RF current of 1.5 mA with a DC bias of 14 mA injected into both sections ($I_a = I_g$). AM efficiency enhancement (Gain Lever) is determined for different values of longer section current (I_g), at various section length ratios. For this analysis, a constant 2.4 GHz RF current is applied to the shorter section biased at 8 mA. The AM efficiency is higher for section length ratio (60/40), when compared to other section length ratios, at this bias point. Higher value of AM efficiency is due to the choice of the operating bias point close to the threshold current, of this section. The value of gain lever variation with longer section current is plotted in Fig. 10.

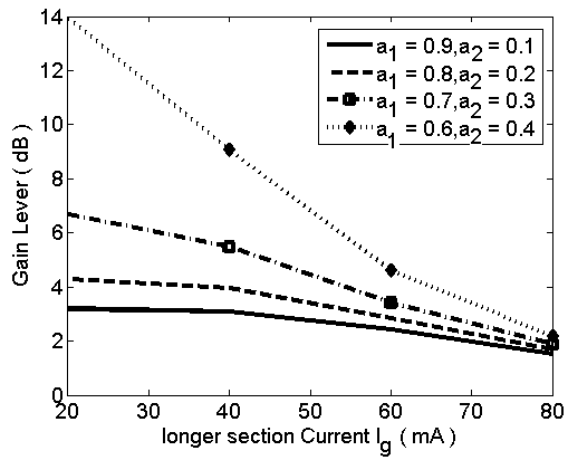


Fig. 10. Gain Lever (AM efficiency enhancement) variation with longer section current (I_g).

From the results, we observe a maximum AM efficiency enhancement of 14 dB for laser diode with section ratio (60/40) at the same bias conditions, when compared to other ratios. It is also inferred that the gain lever reduces for higher value of longer section bias current and the values corresponding to all the section ratios converge to an identical value of AM enhancement at $I_g = 80$ mA and beyond. AM enhancement is higher at lower values of I_g for all the section lengths ratios. Second harmonic distortion (2HD) and third order inter modulation (IMD3) are plotted for same bias conditions and results are compared for all section lengths. These comparisons are shown in Fig. 11 and Fig. 12 respectively.

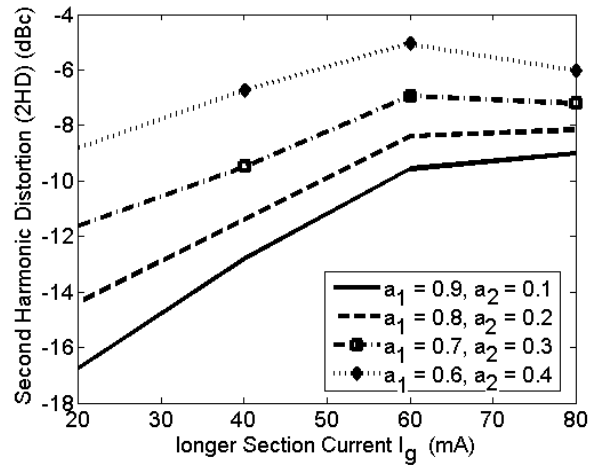


Fig. 11. Second harmonic distortion (2HD) variation with longer section current (I_g).

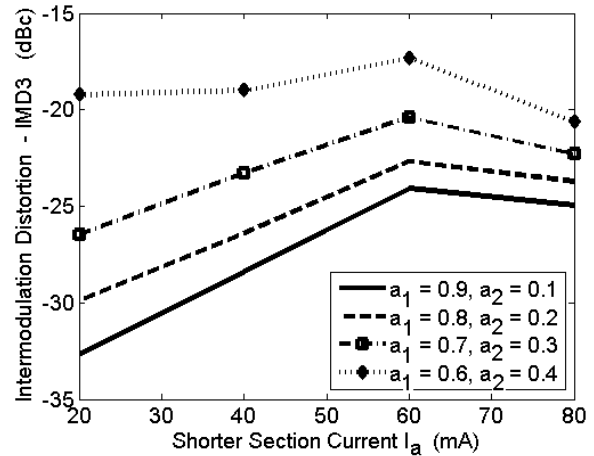


Fig. 12. Third order Inter modulation distortion (IMD3) with longer section current (I_g).

From the above simulations, large gain lever is observed, when the bias currents are close to threshold value of the laser diode, and it decreases at higher bias currents. It has been observed that distortion effects (2HD and IMD3) also become more pronounced when the bias currents are close to threshold current. These distortion effects are found to reduce at higher value of bias conditions. We identify the optimum conditions for gain lever at 2.4 GHz in such devices, i.e., conditions corresponding to minimum distortion and maximum gain lever.

From the results obtained by simulations, optimum values of modulation depth and second harmonic distortion at 2.4 GHz are evaluated and plotted in Fig. 13a. The optimum performances of gain lever laser diode for various section lengths are observed at the bias points corresponding to $I_g = 20$ mA, $I_{a0} = 8$ mA, with the RF current magnitude of 3 mA (I_{a1}). Selection of this bias point is based on large value of modulation depth, gain

lever compared to other bias currents. The maximum value of modulation depth, 15.37 dB and gain lever of 14 dB are obtained for (60/40) device. Minimum second harmonic distortion of -16.75 dBc is observed for (90/10) device. The optimum value of modulation depth and 2HD are obtained as 6.47 dB and -12.96 dBc respectively, for (75/25) device. For the same bias point, third order inter modulation distortion is calculated for various section lengths as described in section 3.2 and plotted in Fig. 13b. The optimum value of IMD3 is observed as -28.5 dBc for (75/25) section length ratio.

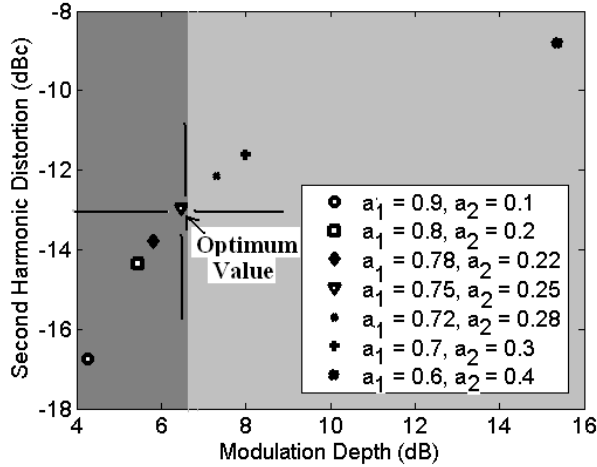


Fig. 13a. Optimum values for Gain lever (dB) and second harmonic distortion (dBc) at $I_g = 20$ mA, $I_a = 8$ mA for 2.4 GHz.

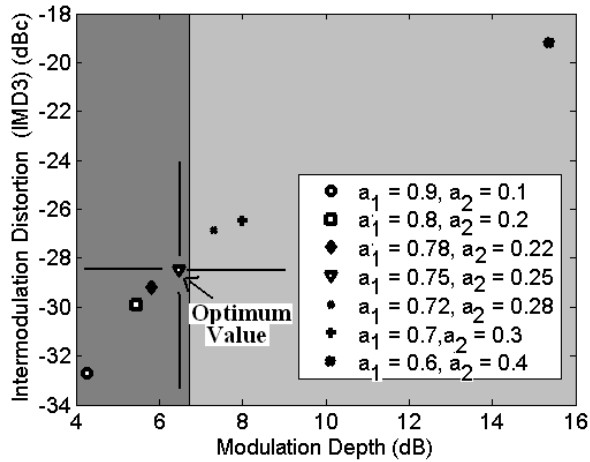


Fig. 13b. Optimum values for Gain lever (dB) and Third order Inter modulation distortion (dBc) at $I_g = 20$ mA, $I_a = 8$ mA for 2.4 GHz.

4. 2. Analysis of harmonic content of optical power

The harmonic contents of optical power output are analyzed for different section lengths by evaluating the expressions obtained from the equations (1)-(4). The value

of longer section and shorter section current is fixed as 20 mA and 8 mA respectively. The static solution of carrier densities and photon density are obtained at this bias point from the equations (11), (12) and (13). The section length ratio is varied from (97/03) to (65/35). The carrier and photon densities are obtained from static solution are used to calculate the first harmonic content of photon density. The first and second harmonic content in carrier densities, photon density and optical power are calculated from equations (14) - (18), at 2.4 GHz. A plot of harmonic contents (Fig. 14) shows an increase of second harmonic content in the output, as the section length ratio varies from (97/03) to (65/35).

The second harmonic distortion is evaluated for different section lengths and plotted in Fig. 15. These values are compared with results obtained from numerical solution. This second harmonic distortion tends to increase as the section length ratio is varied from (97/03) to (65/35). This characteristic is due to the fact that bias point is close to threshold value for section length ratio (60/40) case. The optimum value of second harmonic distortion is found as -13 dBc for a section length ratio of (75/25). This value agrees well with our numerical calculation of second harmonic distortion.

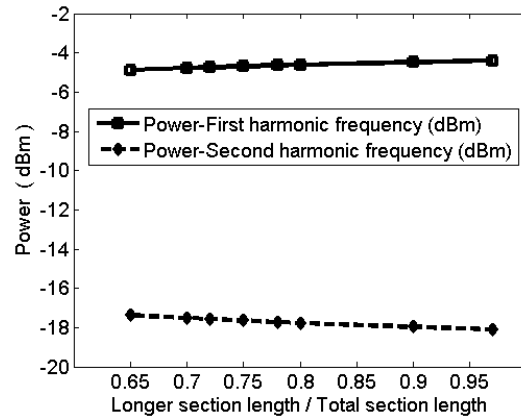


Fig. 14. First and second harmonic content of optical power at $I_g = 20$ mA, $I_a = 8$ mA for 2.4 GHz.

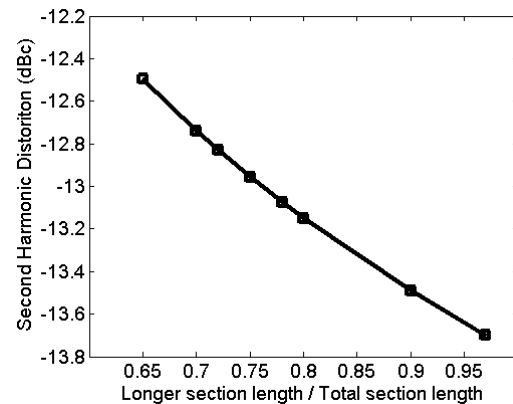


Fig. 15. Second harmonic distortion $I_g = 20$ mA, $I_a = 8$ mA for 2.4 GHz.

5. Conclusions

In this work, we have examined the performance of bi section MQW gain lever laser diode by solving the rate equations in MATLAB®, for DC and dynamic characteristics, under different values of section lengths and section currents. Gain lever (AM enhancement) is calculated at different bias currents at 2.4 GHz RF signal. AM enhancement of 14 dB is obtained for gain lever laser diode with section length (60/40), when biased close to threshold. The effect bias currents and section lengths on the second harmonic distortion (2HD) and third order intermodulation distortion (IMD3) are also analyzed. Optimum values of gain lever corresponding to minimum distortion and condition pertaining, for such values are estimated. First and second harmonic content of optical output is evaluated from the solution of rate equations for various section lengths, and found to agree with results obtained by numerical simulations.

References

- [1] C. H. Cox, G. E. Betts, L. M. Jhonson, IEEE Transactions on Microwave Theory Techniques, **38**, 501(1990).
- [2] Hamed Al-Rawesshidly, Shozo Komaki, Radio Over Fiber Technologies for Mobile Communications Networks, Artech House Inc. (2002).
- [3] M. D. Pocha, L. L. Goddard, T. C. Bond, R. J. Nikolic, S. P. Vernon, J. S. Kallman, E. M. Behymer, IEEE Journal of Quantum Electronics, **43**, 860 (2007).
- [4] K. J. Vahala, M. A. Newkirk, Applied Physics Letters, **54**, 2506 (1989).
- [5] N. Moore, K. Y. Lau, Applied Physics Letters, **55**, 936 (1989).
- [6] C. P. Seltzer, L. D. Westbrook, H. J. Wicks, Electronic Letters, **29**, 230 (1993).
- [7] L. D. Westbrook, C. P. Seltzer, Electronic Letters, **29**, 488 (1993).
- [8] C. P. Seltzer, L. D. Westbrook, H. J. Wicks, IEEE Journal of Lightwave Technology, **13**, 283 (1995).
- [9] Hiroyuki Uenohara, Ryo Takahashi, Yuichi Kawamura, and Hidetoshi Iwamura, IEEE journal of Quantum Electronics, **32**, 873 (1996).
- [10] M. Ganesh Madhan, P. R. Vaya, N. Gunasekaran, IEEE Photonics Technology Letters, **12**, 380 (2000).
- [11] S. J. Zhang, N. H. Zhu, E. Y. B. Pun, P. S. Chung, Microwave and Optical Technology Letters, **49**, 539 (2007).
- [12] W. I. Way, IEEE Lightwave Technology, **5**, 305 (1987).
- [13] H.-K. Sung, M. C. Wu, Journal of optical society of Korea, **12**, 303 (2008).
- [14] F. Rana, C. Monolatou, M. F. Schubert, IEEE Journal of Quantum Electronics, **43**, 1083 (2007).
- [15] H. Zandi, M. Bavafa, M. R. Chamanzar, S. Khorasani, Transaction D: Scientia Iranica, **16**, 145 (2009).
- [16] Geert Morthier, Richard Schatz, Olle Kjebon, IEEE Journal of Quantum Electronics, **36**, 1468 (2000).

*Corresponding author: spsnathan@gmail.com